

Uniaxial pressure induces a Lifshitz phase transition in BaSn_2 : A route to increase the number of topological nodal lines in semimetals

Adolfo O. Fumega,^{1,2,*} Victor Pardo,^{1,2} and A. Cortijo^{3,†}

¹*Departamento de Física Aplicada, Universidade de Santiago de Compostela, E-15782 Campus Sur s/n, Santiago de Compostela, Spain*

²*Instituto de Investigaciones Tecnológicas, Universidade de Santiago de Compostela, E-15782 Campus Sur s/n, Santiago de Compostela, Spain*

³*Departamento de Física de la Materia Condensada, Universidad Autónoma de Madrid, Madrid E-28049, Spain*

Nodal-line semimetal surface states have been proposed to prompt strong correlation effects, such as superconductivity or magnetism. The application of pressure has been demonstrated to induce intriguing phase transitions in these systems. In this work we analyze how uniaxial pressure affects the topological character of BaSn_2 , a Dirac nodal-line semimetal in the absence of spin-orbit coupling. Using calculations based on the density functional theory and a model tight-binding Hamiltonian, we find the emergence of a second nodal line for pressures higher than 4 GPa. Thus, applying pressure increases the number of edge states in the system. We examine the topological features of both phases demonstrating that a nontrivial character is present in both of them. The orbital overlap increase between Ba d_{xz} and d_{yz} orbitals and Sn p_z orbitals is found to be responsible for the advent of this transition. Furthermore, we obtain a topological relation between the zero-energy modes that arise in each phase when a magnetic field is applied.

Introduction.- In the last decades the concept of topology has provided a different perspective to look at materials. This field was initiated with the discovery of topological insulators [1] followed by topological semimetals [2]. Inside the latter category, topological nodal-line semimetals (NLSM) are three dimensional systems in which the valence and conduction bands near the Fermi level cross each other forming a one-dimensional loop in momentum space [3, 4]. These crossings produce nearly flat drumheadlike surface states, which prompt the possibility to study strongly correlated surface phases such as superconductivity or ferromagnetism [5–7].

Topological nodal lines have been reported in the family of ZrSiX materials (where X corresponds to a chalcogen atom) [8–10]. In recent studies, it has been shown that pressure can induce topological phase transitions in these nodal-line semimetals. In the case of ZrSiS , pressure induces a topological nontrivial-to-trivial transition [11], which has been attributed to a weak lattice distortion by nonhydrostatic compression [12]. Infrared spectroscopy experiments have suggested that ZrSiTe undergoes two phase transitions at 4.1 and 6.5 GPa [13]. Raman spectroscopy and X-ray diffraction measurements as well as calculations have found that they correspond to Lifshitz transitions, in which the topology of the Fermi surface changes without breaking any lattice symmetry. Interlayer interactions caused by pressure are found to be responsible of these transitions [14]. However, the topological character of these transitions cannot be elucidated from these experiments. Another question is whether similar transitions appear in other materials hosting NLSM, or instead pressure-induced topological transitions always go in the same direction, from topologically non-trivial to trivial as pressure increases.

BaSn_2 has been reported to be a strong topological insulator with a bulk band gap of about 200 meV [15]. However, in the absence of spin-orbit coupling (SOC) the system becomes a Dirac nodal-line semimetal [16]. It is a layered material that crystallizes in the space group no. 164 (Fig. 1a). Due to this layered structure, it is expected that BaSn_2 is a representative material different from the ZrSiX family to analyze possible pressure-induced topological transitions.

In this work, we study the effect of applying uniaxial pressure to BaSn_2 in the absence of SOC. We have found that at around 4 GPa a Lifshitz transition occurs and a second topological nodal line emerges. We provide a microscopic insight to explain this transition and analyze how it affects the topological properties of BaSn_2 .

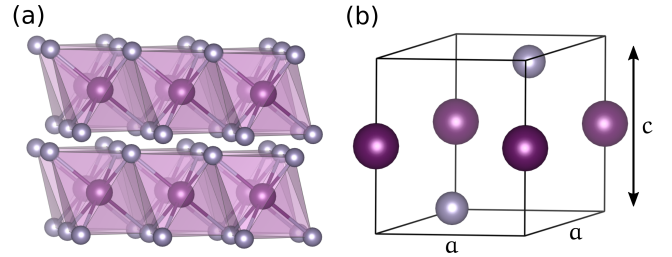


FIG. 1. Crystal structure of BaSn_2 , Ba (Sn) atoms in purple (grey). (a) Side view of the layered structure of BaSn_2 , where Sn atoms octahedrally coordinate the Ba cations. (b) Unit cell of BaSn_2 . Uniaxial pressure is applied along the depicted off-plane c direction.

Discussion.- We start our analysis by performing first principles electronic structure Density Functional Theory (DFT) calculations [17, 18] on BaSn_2 using an all-electron full potential code (WIEN2K) [19]. The exchange-

correlation term was the generalized gradient approximation (GGA) in the Perdew-Burke-Ernzerhof [20] scheme, which properly describes the electronic structure of this system [15, 16]. The calculations were carried out with a converged k -mesh and a value of $R_{mt}K_{max} = 7.0$ and a R_{mt} value of 2.5 a. u. for both Ba and Sn. Uniaxial pressure was imposed by fixing the experimental [21] lattice parameter $a = 4.652 \text{ \AA}$ constant and compressing the c lattice parameter (Fig. 1b). Energy calculations allow us to obtain c as a function of pressure P given in GPa, $c = 5.717 - 0.136P \text{ \AA}$, see Supplementary material. The crystal symmetry is fixed for all the calculations.

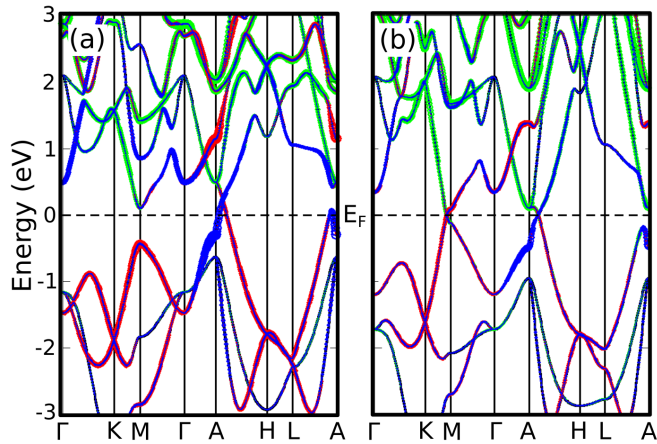


FIG. 2. (Color online) DFT band structures for BaSn₂. The orbital character is highlighted in colors: Sn s in blue, Sn p_z in red and Ba d in green. The Fermi level is set at zero. (a) Band structure for $P = 0$ GPa (T1), there is one band crossing point in the A-H line. (b) Band structure for $P = 6$ GPa (T2), a second band crossing appears near the M point.

Figure 2 shows the DFT band structures of BaSn₂ for two different pressure regimes (SOC is not included). The orbital character of the bands is shown as different colors. At low pressure (Fig. 2a) one band crossing appears in the A-H line. We can see that a band inversion occurs between p_z (in red) and s (in blue) orbitals at that crossing point. The Fermi surface (Fig. 3a) shows that this crossing point corresponds to a topological snake-like nodal line around the A point, with an axis parallel to the z -direction. These main features of the low-pressure phase, that we will call T1, have already been studied in detail in Ref. [16]. The Ba d orbitals (in green in the band structure) are fully unoccupied.

We now turn uniaxial pressure on by reducing the c lattice parameter. The effect in the band structure is that a second crossing point appears along the K-M symmetry line (Fig. 2b). The orbital character of the bands involved in this second crossing is Sn p_z and Ba d , which suggests that a transition to a different phase (T2) might be taking place. The calculation of the Fermi surface (Fig. 3b) shows that this new crossing corresponds to a nodal line around the M point. The plane where this

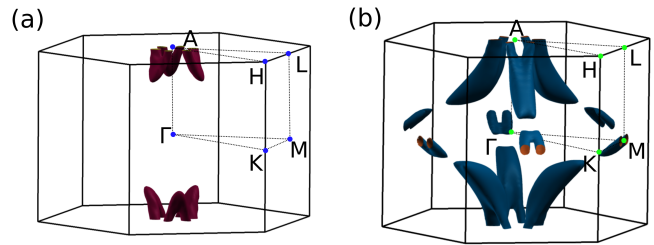


FIG. 3. DFT Fermi surfaces for BaSn₂: (a) for $P = 0$ GPa (T1), it presents a snake-like nodal line around the A point, (b) for $P = 6$ GPa (T2), new nodal lines emerge around the M points.

new nodal line lives is leaned 45° with respect to the z -direction. Since the M point has three arms, three new nodal lines emerge in this new T2 phase.

Note that when SOC is included in these calculations, band crossings are opened and lead to topological insulating states in both phases (see Supplementary material).

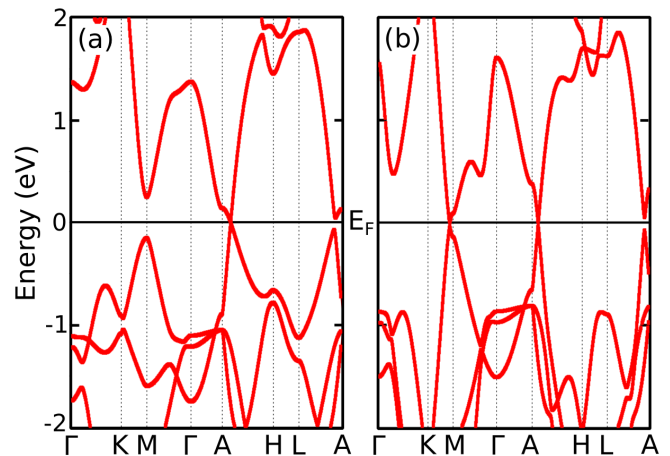


FIG. 4. Tight-binding model band structures for BaSn₂ (a) for $P=0$ GPa (T1), the first band crossing point at the A-H line is well reproduced by the model, (b) for $P=6$ GPa (T2), the second band crossing near the M point is also reproduced.

In order to study the topological features and the microscopic origin of the transition, we have constructed a tight-binding (TB) Hamiltonian as a function of uniaxial pressure. It comprises the s and p orbitals of the two Sn atoms in the unit cell and the d orbitals of the Ba atom (eleven orbitals). Details about the hopping parameters and on-site energies can be seen in the Supplementary material. We have used the PythTB [22] and Pybinding [23] packages to perform the calculations with our TB Hamiltonian. In this TB model the only parameters that depend on pressure are the hopping energies between the Ba d_{xz} and d_{yz} with the Sn p_z orbitals as $t_{d_{xz}p_z} = t_{d_{yz}p_z} = 0.7 + 0.2P$, P being the pressure expressed in GPa and the hoppings in eV. Therefore, the phase transition is thus governed by this particular hop-

ping. It has been previously reported that an increase of interlayer interactions is responsible of the appearance of Lifshitz transitions in ZrSiTe [14]. Here we find that pressure-induced variations in hopping processes within the same Sn-Ba-Sn layer lead to the appearance of a new nodal line.

Figure 4 shows the computed TB band structures for two given pressures below ($P = 0$ GPa) and above ($P = 6$ GPa) the transition. The constructed TB model reproduces fairly well the obtained DFT band structures close to the Fermi level in both phases. The analysis of the TB band crossings is shown in Fig. 5. It can be seen that, in agreement with the DFT calculations, the TB Hamiltonian correctly predicts a snake-like nodal line around the A point for low pressure. For pressures greater than 4 GPa new nodal lines arise around the M points. Again, these are leaned 45° respect to the z -direction.

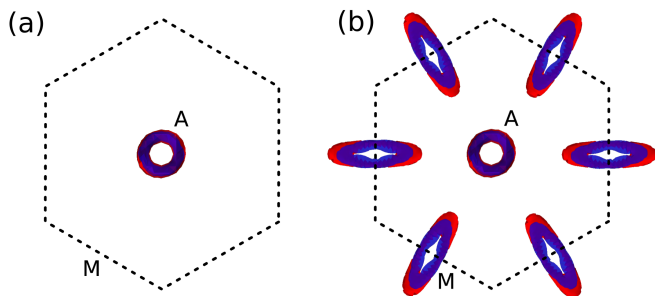


FIG. 5. Top view of the TB band touchings within the first Brillouin zone at the Fermi level. The valence (conduction) band is shown in red (blue): (a) for $P=0$ GPa (T1), the snake-like nodal line is formed around the A point, (b) for $P=6$ GPa (T2), new nodal lines appear around the M points.

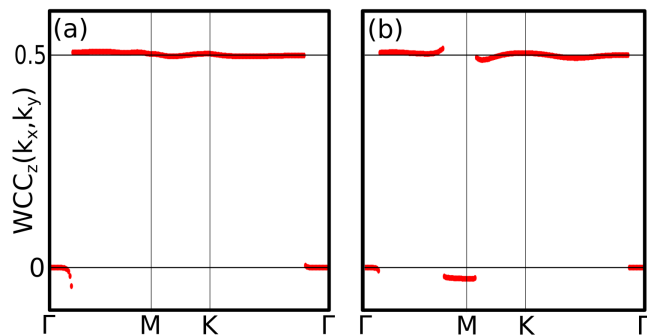


FIG. 6. Wannier charge centers (a) For $P=0$ GPa (T1), around the Γ point and due to the snake-like nodal line a jump of 0.5 happens. (b) For $P=6$ GPa (T2), due to the new topology of the nodal line a second jump of -0.5 appears around the M point.

In order to analyze the nontrivial topological character of the nodal lines, we have computed the sum of the Wannier charge centers along a high symmetry path in the k_x - k_y plane over the z -direction ($\text{WCC}_z(k_x, k_y)$) [24,

25]. This is equal (up to a factor of 2π) to the total Berry phase of the occupied Bloch functions accumulated along the k_z direction, which has to be either 0 or π for an arbitrary loop in the Brillouin zone. Thus, the $\text{WCC}_z(k_x, k_y)$ is expected to be quantized as either 0 or $1/2$ and a jump of $1/2$ will appear when passing through a projected nodal line. At low pressure there is only one nodal line around the A point, which produces a jump of $1/2$ in $\text{WCC}_z(k_x, k_y)$ when crossing it (see Fig. 6a). This confirms the topological character of that nodal line, as already reported in Ref. 16. In the high pressure regime new nodal lines emerge around the M points. It can be observed in Fig. 6b that they produce a jump of $-1/2$ in $\text{WCC}_z(k_x, k_y)$. This is a proof of the nontrivial character also for these nodal lines. Note, however, that nodal lines around the M points have opposite sign to that around A. Since the M point has 3 branches it contributes three times. Adding contributions from all the nodal lines the system at high pressures behaves as it would have two nodal lines, i.e., this phase transition has increased the amount of topological nodal lines by 1.

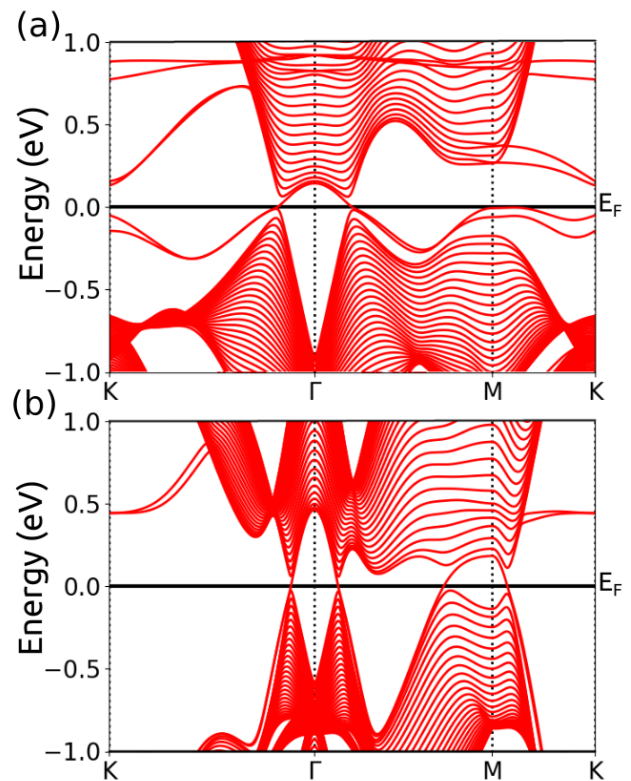


FIG. 7. Energy states in a 30-layer structure stacked along the z -direction (Sn-dangling bond terminated). (a) For $P=0$ (T1), a surface state crosses the Fermi level around the Γ point, this state is associated to the snake-like nodal line (b) For $P=6$ GPa (T2), a second surface state crossing appears around the M point due to the new nodal lines.

As mention above, one important feature of the topological NLSM is their drumhead-like surface states. The

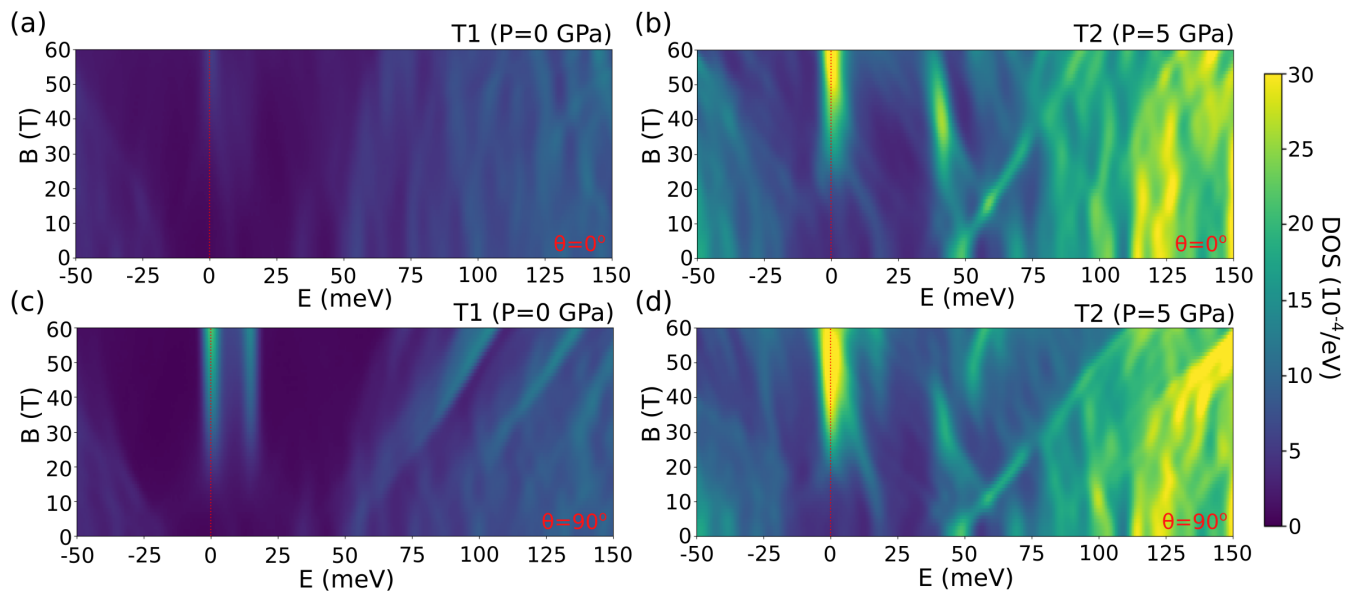


FIG. 8. Colormap of the density of states as a function of an applied magnetic field B along the z -direction (a,b) and perpendicular to it (c,d) for the T1 phase (a,c) and for the T2 phase (b,d). Magnetic oscillations and zero-energy modes are analyzed in the text.

TB Hamiltonian allows us to compute them in each phase. Figure 7a shows the energy states of a 30-layer structure stacked along the z -direction for the T1 phase, i.e. at low pressures. Metallic edge states associated to the nodal line around A can be seen projected around Γ . In the high pressure T2 phase, new metallic surface states emerge around M (Fig. 7b), which are related to the new nodal lines. Moreover, the dispersion of all surface states is increased by uniaxial pressure. In the case of the snake-like nodal line, in the T1 phase the bandwidth of the surface state is about 0.2 eV, while in the T2 phase it increases to become almost 1 eV. Note also that the surface states are highly sensitive to the kind of truncation imposed to the structure. Here we chose to terminate with a Sn-rich plane for our calculations, but different cuts can be used to obtain surface states inside or outside the projected nodal loop as explained in Ref. [16].

Magnetotransport measurements are the most extended experimental tests employed to analyze the topological character of NLSM through the analysis of the corresponding Landau level fan diagrams. It is also known that the same information can be obtained from quantum oscillations in the density of states (DOS) [26–28]. Together with the Berry phase contribution to the phase of the quantum oscillations, non-trivial topological phases in NLSM are characterized by the appearance of zero-energy Landau levels [29] in the presence of a magnetic field. The orbits associated to this zero-energy Landau level would be in turn responsible for the presence of a nontrivial Berry phase in the Landau level fan diagram.

Therefore, we have included a magnetic field (B) in our TB Hamiltonian through a Peierls flux with 80 unit cells in each direction. The kernel polynomial method [30] was used to compute the DOS as a function of the applied magnetic field (Fig. 8).

In the low-pressure regime T1, there is only one nodal loop, lying in the OZ plane. When the magnetic field is applied perpendicularly to the nodal line ($\theta = 0$), no zero-energy modes are present since all the magnetic oscillations are trivial (Fig. 8a). However, when the field is applied perpendicular to the OZ plane ($\theta = \pi/2$) the DOS associated to a zero-energy Landau level is observed (Fig. 8c). These results are in agreement and equivalent to those of a single nodal line lying in the k_x - k_y plane produced by a cubic lattice [27].

In the high-pressure phase T2, new nodal lines tilted $\pi/4$ respect the OZ -direction are present around the M points. Thus, when the magnetic field is applied along the OZ -direction ($\theta = 0$) only the contribution from these new nodal lines is observed in the DOS at zero energy (Fig. 8b). The presence of this zero-energy mode is related with the nontrivial Berry phase that can be measured by the analysis of the quantum oscillations in magnetotransport. When B is applied perpendicular to the OZ plane ($\theta = \pi/2$), the original nodal line and the new ones contribute to the DOS at $E = 0$. Since both zero-energy modes correspond to an extreme orbit that dominates the amplitude of the quantum oscillations, we expect a substantial increase in the magneto-oscillation amplitude (Fig. 8d). We are focusing on the qualitative analysis of the pressure-induced topological phase transi-

tions in NLSM, a fully quantitative analysis of the topological character of the quantum oscillations goes beyond the scope of the present work. However, we can obtain more quantitative results by focusing on the features of the zero-energy DOS of each phase.

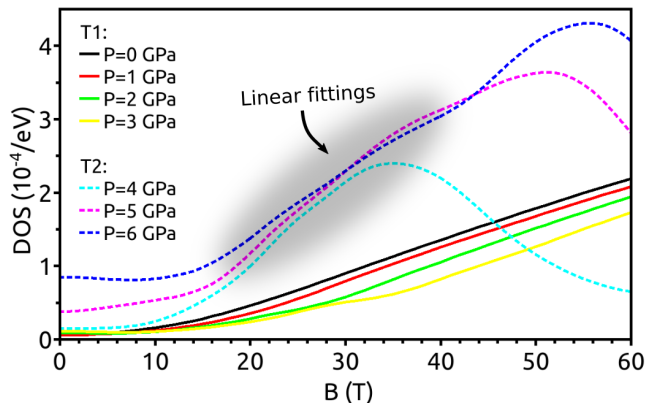


FIG. 9. Zero-energy modes for different pressures as a function of the magnetic field. Linear fittings were performed for each phase. The ratio between slopes is 1.98, demonstrating the existence of a topological-to-topological phase transition (see text).

Figure 9 shows the DOS at zero energy as a function of B , for $\theta = \pi/2$ and for different pressure values. Both phases can be identified in this plot. While in the T1 phase there is only one nodal line contributing to the DOS at the Fermi level, in the T2 phase the emergence of 3 new nodal lines with opposite sign (as previously shown in the $WCC_z(k_x, k_y)$ analysis) makes the system behave as it would have 2 independent nodal lines. Therefore, the DOS at the Fermi level in the T2 phase is expected to be two times that in the T1 phase. To check whether this argument is correct, we have performed linear fittings of the DOS as a function of B . While the dependence of the DOS with B in the T1 phase is almost linear since there is only 1 nodal line, the behavior in the T2 phase appears to be more complex as there are multiple nodal lines oriented along different directions. For this reason, we have restricted the fittings to a range of values in which the DOS shows a linear trend (shaded area in Fig. 9). We have also averaged the slopes of each phase to reduce the uncertainty. We have obtained a ratio between the slope of phase T2 (s_{T2}) and T1 (s_{T1}) of $s_{T2}/s_{T1} = 1.98 \simeq 2$. Therefore, this demonstrates a clear signature of a topological-to-topological phase transition.

Conclusions.- It has been widely reported, both theoretically and experimentally, that pressure can induce changes in the Fermi surface of different materials [31–34], and in some cases pressure has been found to modify the topological character of the compound. For instance, it has been shown that pressure can induce a transition to a nontrivial topological phase from a trivial one [35–

41]. The opposite case has been reported too. Pressure is able to induce a transition from topological to trivial in which topological objects such as nodal pairs [42] or nodal lines are annihilated [11]. In our work, we report a different kind of transition (topological-to-topological) in BaSn_2 when SOC is neglected. We have shown that pressure can increase the number of topological nodal lines in an already nontrivial compound.

Our DFT calculations show that for uniaxial pressures along the z -direction greater than 4 GPa new nodal lines emerge in the Dirac NLSM BaSn_2 . The topological character of these new nodal lines was studied with a model TB Hamiltonian that reproduces the DFT calculations as a function of pressure. The analysis of the $WCC_z(k_x, k_y)$, surface states and zero-energy modes when a magnetic field is applied, demonstrate that BaSn_2 undergoes a topological to topological phase transition at around 4 GPa. Multiorbital character of the bands and crystal symmetry preservation have been found to be important factors to increase the number of topological nodal lines. In the present case, we propose a way to experimentally test this kind of topological-to-topological transition by noticing that the observation of the Berry phase in the fan diagram strongly depends on the tilting angle θ between the magnetic field and the nodal line [27]. Thus, for a given tilting angle θ where the magneto-oscillations appear to be trivial, the appearance of another nodal line with different tilting angle with respect to the magnetic field will generate topologically nontrivial magneto-oscillations, and thus providing a way to directly observe the topological transition described in the present work.

Acknowledgements.- This work is supported by the MINECO of Spain through the project PGC2018-101334-B-C21. A.O.F. thanks MECD for the financial support received through the FPU grant FPU16/02572. A.C. acknowledges financial support through MINECO/AEI/FEDER, UE Grant No. FIS2015-73454-JIN and European Union structural funds, the Comunidad Autónoma de Madrid (CAM) NMAT2D-CM Program (S2018-NMT-4511), and the Ramón y Cajal program through the grant RYC2018-023938-I. A. C. acknowledges useful discussions with Laszlo Oroszlany.

* adolfo.otero.fumega@usc.es

† alberto.cortijo@uam.es

- [1] M. Z. Hasan and C. L. Kane, *Rev. Mod. Phys.* **82**, 3045 (2010).
- [2] N. P. Armitage, E. J. Mele, and A. Vishwanath, *Rev. Mod. Phys.* **90**, 015001 (2018).
- [3] V. Pardo and W. E. Pickett, *Physical Review B* **81**, 245117 (2010).
- [4] A. A. Burkov, M. D. Hook, and L. Balents, *Phys. Rev.*

- B 84**, 235126 (2011).
- [5] N. B. Kopnin, T. T. Heikkilä, and G. E. Volovik, *Phys. Rev. B* **83**, 220503 (2011).
- [6] W. Chen and J. L. Lado, *Phys. Rev. Lett.* **122**, 016803 (2019).
- [7] Y. Shao, A. N. Rudenko, J. Hu, Z. Sun, Y. Zhu, S. Moon, A. J. Millis, S. Yuan, A. I. Lichtenstein, D. Smirnov, Z. Q. Mao, M. I. Katsnelson, and D. N. Basov, *Nature Physics* (2020), 10.1038/s41567-020-0859-z.
- [8] L. M. Schoop, M. N. Ali, C. Straßer, A. Topp, A. Varykhalov, D. Marchenko, V. Duppel, S. S. P. Parkin, B. V. Lotsch, and C. R. Ast, *Nature Communications* **7**, 11696 (2016).
- [9] J. Hu, Z. Tang, J. Liu, X. Liu, Y. Zhu, D. Graf, K. Myhro, S. Tran, C. N. Lau, J. Wei, and Z. Mao, *Phys. Rev. Lett.* **117**, 016602 (2016).
- [10] M. Neupane, I. Belopolski, M. M. Hosen, D. S. Sanchez, R. Sankar, M. Szlawaska, S.-Y. Xu, K. Dimitri, N. Dhakal, P. Maldonado, P. M. Oppeneer, D. Kaczorowski, F. Chou, M. Z. Hasan, and T. Durakiewicz, *Phys. Rev. B* **93**, 201104 (2016).
- [11] D. VanGennep, T. A. Paul, C. W. Yerger, S. T. Weir, Y. K. Vohra, and J. J. Hamlin, *Phys. Rev. B* **99**, 085204 (2019).
- [12] C. C. Gu, J. Hu, X. L. Chen, Z. P. Guo, B. T. Fu, Y. H. Zhou, C. An, Y. Zhou, R. R. Zhang, C. Y. Xi, Q. Y. Gu, C. Park, H. Y. Shu, W. G. Yang, L. Pi, Y. H. Zhang, Y. G. Yao, Z. R. Yang, J. H. Zhou, J. Sun, Z. Q. Mao, and M. L. Tian, *Phys. Rev. B* **100**, 205124 (2019).
- [13] J. Ebad-Allah, M. Krottenmüller, J. Hu, Y. L. Zhu, Z. Q. Mao, and C. A. Kuntscher, *Phys. Rev. B* **99**, 245133 (2019).
- [14] M. Krottenmüller, M. Vöst, N. Unglert, J. Ebad-Allah, G. Eickerling, D. Volkmer, J. Hu, Y. L. Zhu, Z. Q. Mao, W. Scherer, and C. A. Kuntscher, *Phys. Rev. B* **101**, 081108 (2020).
- [15] S. M. Young, S. Manni, J. Shao, P. C. Canfield, and A. N. Kolmogorov, *Phys. Rev. B* **95**, 085116 (2017).
- [16] H. Huang, J. Liu, D. Vanderbilt, and W. Duan, *Phys. Rev. B* **93**, 201114 (2016).
- [17] P. Hohenberg and W. Kohn, *Phys. Rev.* **136**, B864 (1964).
- [18] W. Kohn and L. J. Sham, *Phys. Rev.* **140**, A1133 (1965).
- [19] K. Schwarz and P. Blaha, *Comp. Mater. Sci.* **28**, 259 (2003).
- [20] J. P. Perdew, K. Burke, and M. Ernzerhof, *Phys. Rev. Lett.* **77**, 3865 (1996).
- [21] S.-J. Kim and T. F. Fessler, *Zeitschrift für Kristallographie - New Crystal Structures* **223**, 325 (2008).
- [22] D. Vanderbilt, “The pythtb package,” in *Berry Phases in Electronic Structure Theory: Electric Polarization, Orbital Magnetization and Topological Insulators* (Cambridge University Press, 2018) p. 327362.
- [23] D. Moldovan, M. Anelkovi, and F. Peeters, “pybinding v0.9.4: a Python package for tight-binding calculations,” (2017), This work was supported by the Flemish Science Foundation (FWO-VI) and the Methusalem Funding of the Flemish Government.
- [24] R. Yu, X. L. Qi, A. Bernevig, Z. Fang, and X. Dai, *Phys. Rev. B* **84**, 075119 (2011).
- [25] M. Taherinejad, K. F. Garrity, and D. Vanderbilt, *Phys. Rev. B* **89**, 115102 (2014).
- [26] C. Li, C. M. Wang, B. Wan, X. Wan, H.-Z. Lu, and X. C. Xie, *Phys. Rev. Lett.* **120**, 146602 (2018).
- [27] L. Oroszlány, B. Dóra, J. Cserti, and A. Cortijo, *Phys. Rev. B* **97**, 205107 (2018).
- [28] H. Yang, R. Moessner, and L.-K. Lim, *Phys. Rev. B* **97**, 165118 (2018).
- [29] J.-W. Rhim and Y. B. Kim, *Phys. Rev. B* **92**, 045126 (2015).
- [30] A. Weiße, G. Wellein, A. Alvermann, and H. Fehske, *Rev. Mod. Phys.* **78**, 275 (2006).
- [31] S. Ram, V. Kanchana, G. Vaitheeswaran, A. Svane, S. B. Dugdale, and N. E. Christensen, *Phys. Rev. B* **85**, 174531 (2012).
- [32] J. Zhang, C. Liu, X. Zhang, F. Ke, Y. Han, G. Peng, Y. Ma, and C. Gao, *Applied Physics Letters* **103**, 052102 (2013), <https://doi.org/10.1063/1.4816758>.
- [33] Y. Zhang, X. Shao, Y. Zheng, L. Yan, P. Zhu, Y. Li, and H. Xu, *Journal of Alloys and Compounds* **732**, 280 (2018).
- [34] Y. Zhang, Y. Li, Y. Ma, Y. Li, G. Li, X. Shao, H. Wang, T. Cui, X. Wang, and P. Zhu, *Scientific Reports* **5**, 14681 (2015).
- [35] W. Li, X.-Y. Wei, J.-X. Zhu, C. S. Ting, and Y. Chen, *Phys. Rev. B* **89**, 035101 (2014).
- [36] W. Liu, X. Peng, C. Tang, L. Sun, K. Zhang, and J. Zhong, *Phys. Rev. B* **84**, 245105 (2011).
- [37] J. Zhou, S. Zhang, and J. Li, *NPG Asia Materials* **12**, 2 (2020).
- [38] V. Rajaji, R. Arora, S. C. Sarma, B. Joseph, S. C. Peter, U. V. Waghmare, and C. Narayana, *Phys. Rev. B* **99**, 184109 (2019).
- [39] P.-J. Guo, H.-C. Yang, K. Liu, and Z.-Y. Lu, *Phys. Rev. B* **96**, 081112 (2017).
- [40] T. Teshome and A. Datta, *ACS Omega* **4**, 8701 (2019).
- [41] Y. Xia and G. Li, *Phys. Rev. B* **96**, 241204 (2017).
- [42] C. Zhang, J. Sun, F. Liu, A. Narayan, N. Li, X. Yuan, Y. Liu, J. Dai, Y. Long, Y. Uwatoko, J. Shen, S. Sanvito, W. Yang, J. Cheng, and F. Xiu, *Phys. Rev. B* **96**, 155205 (2017).